Title: **Direct Ab-initio Molecular Dynamics (AIMD) Study on the Radiation Effects on Catalytic Triad composed of Ser-His-Glu residues**

Authors: Hiroto TACHIKAWA* and Hiroshi KAWABATA[#]

Division of Materials Chemistry, Graduate School of Engineering, Hokkaido University, Kita-ku, Sapporo 060-8628, JAPAN

[#]*Young Researchers Education Center*
Hiroshima University, Higashihiroshima, 739-8512, JAPAN

Manuscript submitted to: *International Journal of Quantum Chemistry*
Section of the journal: *Article*

Correspondence and Proof to: Dr. Hiroto TACHIKAWA*
Division of Applied Chemistry
Graduate School of Engineering
Hokkaido University
Sapporo 060-8628, JAPAN
hiroto@eng.hokudai.ac.jp
Fax. +81 11706-7897

Contents :

Graphical abstract

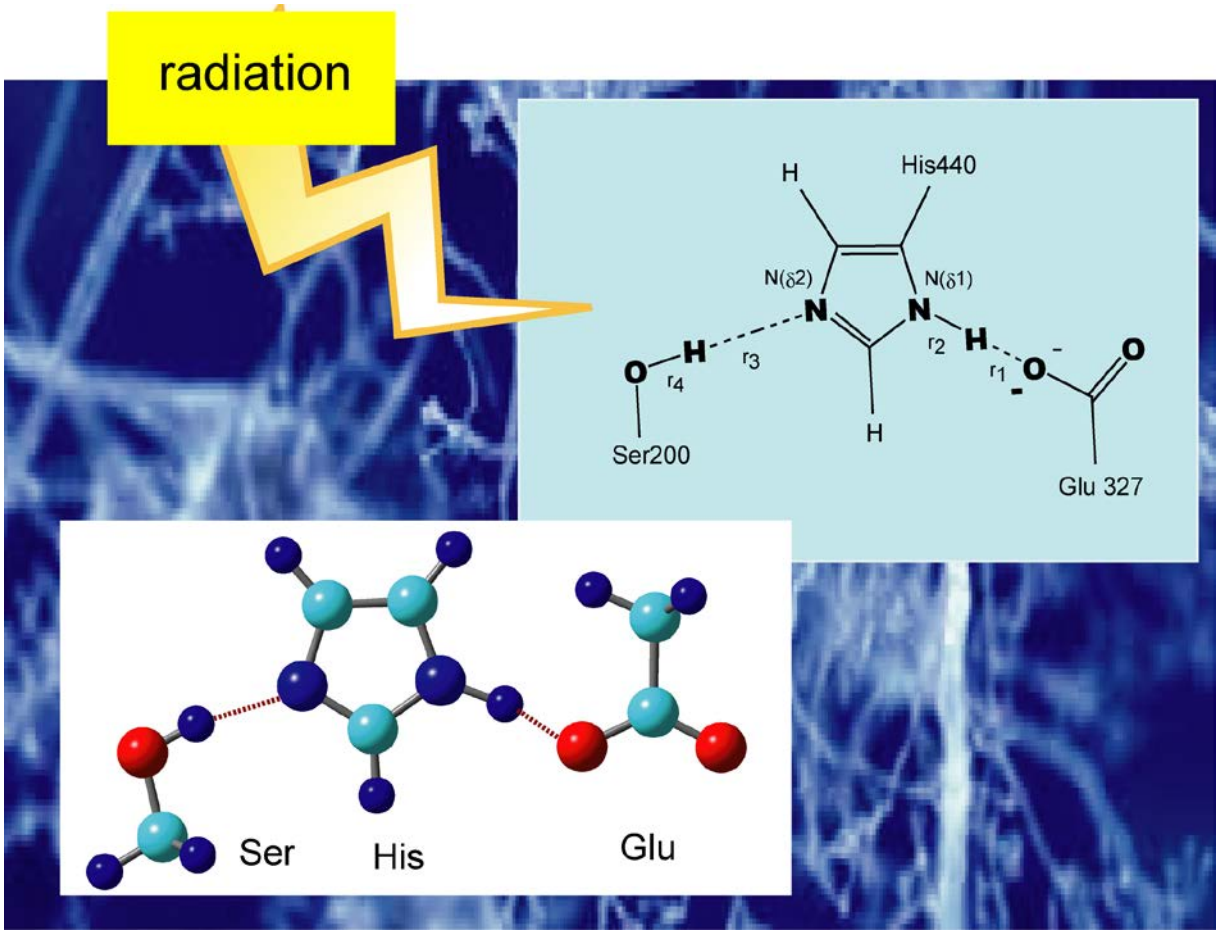

2015_09_04_revised

Direct Ab-initio Molecular Dynamics (AIMD) Study on the Radiation Effects on Catalytic Triad composed of Ser-His-Glu residues

Hiroto TACHIKAWA* and Hiroshi KAWABATA[#]

Division of Applied Chemistry, Graduate School of Engineering,
Hokkaido University, Sapporo 060-8628, JAPAN
[#]Young Researchers Education Center
Hiroshima University, Higashihiroshima, 739-8512, JAPAN

Abstract: High energy irradiation to the hydrogen bonded system is important in relevance with the initial process of DNA and enzyme damages. In the present study, the effects of radiation to catalytic triad have been investigated by means of direct ab-initio molecular dynamics (AIMD) calculation. As a model of the catalytic triad, Ser-His-Glu residue, which is one of the important enzymes in the acylation reaction, was examined. The ionization and electron attachment processes in Ser-His-Glu were investigated as the radiation effects,. The direct AIMD calculation showed that a proton of His is spontaneously transferred to carbonyl oxygen of Glu after the ionization. However, the whole structure of catalytic triad was essentially kept after the ionization. On the other hand, in the case of the electron capture in the model catalytic triad Ser-His-Glu, the dissociation of Glu residue from $[Ser\text{-}His]^-$ was found as a product channel. The mechanism of ionization and electron capture process in the catalytic triad was discussed on the basis of theoretical results.

Keywords: Proton transfer; Ionization; Electron capture; Degradation of catalytic triads; cluster

1. Introduction

High energy irradiation to the hydrogen bonded system is important in relevant with the initial process of DNA damages [1-3] and enzyme damages [4-7]. If DNA base pair is ionized by the irradiation, a proton is transferred into the neighbored base along the hydrogen bond, while a defect is formed in the damaged DNA [8,9]. The defect leads to replication and transcriptional errors in DNA.

Many experimental and theoretical works on the DNA damage have been carried out in last decade [1-3,8,9]. On the other hand, the studying of radiation enzyme damages is limited.[4-7] Acetylcholinesterase (AChE) is one of the enzymes which is composed of catalytic triad in the active site consisting of the amino acids, serine (Ser), histidine (His), and glutamic acid (Glu) [10-12]. AChE can synthesize neurotransmitter acetylcholine (ACh) by the transition of acetyl groups of acetyl CoA [13-15]. The reaction efficiency of AChE is significantly larger than the other enzymes. The change of ACh into choline and acetic acid by AChE proceeds in two stages, aceylation and deacetylation. In the case of human AChE, Ser200 and His440 in the active site are involved in the reaction with substrate ACh during the AChE catalysis. The reaction proceeds after the proton transfer from Ser200 to imidazole of His440 and nucleophilic addition of the oxygen atom of Ser200 to the substrate ACh occurs subsequently [16-23]. Thus, the catalytic triad plays an important role in human synthesize neurotransmitter. However, there is no study on the radiation effects to Ser-His-Glu.

In the present study, the radiation damage of catalytic triad Ser200-His400-Glu327 is investigated theoretically by means of direct ab-initio molecular dynamics (AIMD) method As the radiation damage to the catalytic triad, ionization (hole capture) and electron capture processes of Ser200-His400-Glu327 were examined in the present work.

2. Computational section

A. Structural model of catalytic triad

Enzyme in human acetylcholinesterase (AChE) is composed of catalytic triad consisted of Ser200, His440, and Glu327. In the present study, these residues, Ser200, His440 and Glu327, were modeled by CH_3OH, $C_3N_2H_4$, and CH_3COO^-, respectively. This model of the catalytic triad is expressed hereafter by Ser-His-Glu. The charges and multiplicity of Ser-His-Glu were -1 and singlet state, respectively. First, we carried out the geometry optimizations of the catalytic triad at the MP2/6-311++G(d,p) level of theory. Note that the optimized structure of the model catalytic triad was close to the structure obtained by X-ray experiment for native enzyme (*T.california*) [24]. Schematic illustration of the model of the catalytic triad and the geometric parameters for the model are given in Figure 1. All static ab-initio calculations were carried out using GAUSSIAN09 program package [25].

B. Direct ab-initio molecular dynamics (AIMD) calculation

The structure of the catalytic triad was optimized at the MP2/6-311++G(d,p) level of theory. The direct AIMD calculation [26-28] was carried out from the optimized structure of Ser-His-Glu. We used complete active space-self consistent field theory (CAS-SCF) to calculate electronic structures and multi-dimensional potential energy surface for the cation and anion systems [29]. Three electron and three molecular orbitals were considered as the active electron and active space, respectively. The active spaces of $[Ser\text{-}His\text{-}Glu]^+$ and $[Ser\text{-}His\text{-}Glu]^-$ were chosen as (HOMO-1, HOMO, LUMO) and (HOMO, LUMO, LUMO-1) of [Ser-His-Glu], respectively. The spatial distributions of active orbitals in the CAS calculation are illustrated in Figure S1 in supporting information. The vertical ionization and

electron capture from Ser-His-Glu were assumed at time zero. The charges and multiplicities of [Ser-His-Glu], $[Ser\text{-}His\text{-}Glu]^+$ and $[Ser\text{-}His\text{-}Glu]^-$ were (charge, multiplicity)=(-1, singlet), (0, doublet), and (-2, doublet), respectively. Note that [Ser-His-Glu] and $[Ser\text{-}His\text{-}Glu]^-$ are neutral radical and dianion, respectively.

In addition to the trajectory from the optimized geometry of Ser-His-Glu, five trajectories were selected and run from the Franck-Condon (FC) region of Ser-His-Glu. The sampling method was described in our previous papers [30,31]. The equations of motion were numerically solved by the velocity Verlet algorithm method [32]. No symmetry restriction was applied to the calculation of the energy gradients. The time step size was chosen to be 0.10 fs, and a total of 1500-2000 steps were calculated for each calculation. The trajectory calculations were performed under condition of constant total energy (=kinetic energy + potential energy). The momentum of the center of mass and the angular momentum were assumed to zero at time zero. To check the CAS(3,3) results, direct AIMD calculations were carried out at the CAS(5,5) and MP2 levels of theory.

3. Results

A. Structures of catalytic triad

First, we carried out the geometry optimizations of the catalytic triad composed of Ser-His-Glu at the MP2/6-311++G(d,p) level of theory. The optimized structure is illustrated in Figure 1. The intermolecular hydrogen bond distances for His-Glu and Ser-His were calculated to be r_1=1.435 Å and r_3= 1.837 Å, respectively. The geometrical parameter (r_1) is defined by the distance of the hydrogen bond between the NH proton of His N1 and oxygen atom of Ser, while r_3 is defined by the distance between the nitrogen atom N2 of His and hydrogen atom of Ser. The geometrical parameters (r_2 and r_4) are defined by the N1-H bond of

His and O-H bond of Ser, respectively. The proton transfer can be expressed by change of these parameters. For example, the decrease of r_1 and increase of r_2 mean the proton transfer from His440 to Glu, and the decrease of r_3 and increase of r_4 mean a proton transfer from Ser to His. At time zero, the NH bond length of His is r_2=1.095 Å, and His was located at r_1=1.518 Å from the oxygen atom of Glu.

B. Hole capture (ionization) dynamics of Ser-His-Glu

The result for a sample trajectory for the ionization of Ser-His-Glu is given in Figure 2. At time zero, an electron was vertically removed from the reaction system. The proton of His was located at r_1=1.518 Å from the oxygen atom of Glu and at r_2=1.095 Å from the nitrogen atom of His (N1). Ser was located at 1.879 Å (=r_3) from His as a hydrogen bond distance. The N1-H bond distance was r_2=1.095 Å and the angle of N-H-O was θ_2=169.9° at time zero. After 7.0 fs, the proton approached rapidly to the oxygen atom of Glu (O1) with r_1=1.265 Å and r_2=1.343 Å, while the N-H-O angle was 171.1°. At time=9.0 fs, the O-H bond was newly formed in the Glu residue (r_1=0.927 Å). The N-H distance was r_2=1.662 Å. The proton vibrated between the oxygen atom of Glu and nitrogen of His (N1) after the proton transfer. The intermolecular distances (N1-O) at time = 0, 7, and 9 fs were 2.603, 2.600, and 2.580 Å, respectively, indicating that the proton is only transferred from His to Glu with a fixed His-Glu intermolecular distance. The angle of N1-H-O1 (θ_2) was almost constant during the proton transfer, indicating that the proton transfer takes place with collinear form. After 40 fs, the formation of O-H bond was fully completed, and acetic acid CH_3COOH was formed as the final product.

The positions of Ser at time = 0, 7, 9, and 40 fs were 2.863, 2.893, 2.905, 2.984 Å as N2-O2 distance, respectively. The distances of hydrogen bond between Ser and His at 0, 7, 9, and 40

fs were r_3 = 1.879, 1.936, 1.944, and 2.054 Å, respectively. The structural change indicates that Ser leaves slightly from His after the ionization due to the repulsive interaction between His^+ and the proton of Ser.

At the final stage of the ionization (time=105 and 160 fs), the distance of hydrogen bond between Ser-His was r_3=2.369 Å (105 fs) and 2.427 Å (160fs), indicating that Ser leaves gradually from His. The excess energy generated by the reaction was dissipated into the translational energy of Ser. The O2-H distances (=r_4) becomes shorter as time is increased. This is due to the fact that the hydrogen bond becomes weaker at longer separation.

As well as behavior of Ser, Glu added by the proton leaved gradually from His: the distances of r_2 at time=0, 7, 9, 40, 105, and 160 fs were 1.095, 1.343, 1.662, 1.817, 2.322, and 2.642 Å. The excess energy was also transferred into the translational mode of Glu. These results indicate that the hydrogen bonded structure of Ser-His-Glu is gradually destroyed after the proton transfer.

Thus, the reaction can be summarized as follows. After the hole capture, the proton of His is directly transferred to Glu without activation barrier. This transfer is a very fast process. The skeleton structure was kept during the proton transfer. The hydrogen bonded structure of Ser-His-Glu is gradually destroyed after the proton transfer. A total of five trajectories were run as the vertical ionization process of Ser-His-Glu. All calculations gave the similar results.

C. Potential energy curve for the proton transfer from His^+ to Glu

In previous section, it was found that the proton is directly transferred from His^+ to Glu after the hole capture of Ser-His-Glu. The potential energy curves (PECs) along the proton transfer coordinate are given in Figure 3. The calculations were carried out at the CAS(3,3)/6-31G(d), CAS(5,5)/6-31G(d), MP2/6-311G(d,p), and MP2/6-311++G(d,p) levels

of theory. The horizontal line in r(N-H)=1.1 Å indicates the vertical ionization point of Ser-His-Glu. The zero level of the energy corresponds to this line. The proton transfer proceeds as an exthothermic reaction with ΔH= -23 kcal/mol. All calculations showed that the proton transfer takes place without barrier.

It was found that PEC calculated by CAS(3,3) was close to that of CAS(5,5). Also, the shape of PEC was reasonably agreed with those of MP2 calculation. These results indicate that direct AIMD calculation at the CAS(3,3) would give a reasonable result for the reaction dynamics of Ser-His-Glu.

D. Electron capture dynamics of Ser-His-Glu.

Snapshots of $[Ser\text{-}His\text{-}Glu]^-$after the electron capture are illustrated in Figure 4. At time zero (point a), Ser and Glu were located at r_3=1.812 Å and r_1=1.505 Å from His, respectively. After the electron capture of Ser-His-Glu, the excess electron was mainly localized on His. At 60 fs (point b), Glu was located at r_1=2.380 Å, indicating that Glu leaves from His. On the other hand, Ser approached to His: the distances of Ser from His at time =0 and 60 fs were 1.812 and 1.588 Å, respectively. This approach is caused by attractive interaction between negatively charged His and proton of Ser.

At 128 fs (point c), Glu and Ser were located in r_1 =3.821 Å and r_3=1.754 Å. The intermolecular distances between His^- and Glu at time=0, 60, 128, and 180 fs were $r(N_1\text{-}O_1)$=2.584, 3.423, 4.769, and 6.086 Å, respectively, indicating that the Glu is monotonically decreased after the electron capture of Ser-His-Glu. The dissociation was caused by repulsive interaction between negatively charged His^- and CH_3OO^-. Skeleton structure of His was varied gradually after the electron capture. Especially, the C1-N1 bond of His was changed from 1.343 Å (time=0) to 1.470 Å (146 fs).

The reaction can be summarized as follows. After the electron capture of Ser-His-Glu, the Glu leaves from His due to the repulsive interaction of His^- and $Glu\text{-}COO^-$. The hydrogen bond between His-Ser is still connected. The proton of His is not transferred to Glu. A total of five trajectories were run as the vertical ionization process of Ser-His-Glu. All calculations gave the similar results.

E. Time evolution of potential energy

To elucidate the reaction dynamics in more details, the potential energies of Ser-His-Glu after the hole and electron captures are given in Figure 5. In the hole capture, the potential energy decreased suddenly to -36 kcal/mol at 0-9 fs (points a → b → c). This energy change was caused by the fast proton transfer from His to Glu. After the proton transfer, the potential energy vibrated strongly, while the O-H bond in Glu was newly formed. The strong oscillation was originated from the O-H stretching vibration. The proton transfer was completed at 20-30 fs.

The potential energy curve for electron capture was significantly different from that in hole capture. The potential energy decreased slowly: potential energies were -12 kcal/mol (20 fs), and -25 kcal/mol (110 fs), respectively. Around 150 fs, the dissociation was almost completed (-32 kcal/mol).

F. Spin densities on catalytic triad

The spin densities on $[Ser\text{-}His\text{-}Glu]^+$ and $[Ser\text{-}His\text{-}Glu]^-$ at time zero (i.e., vertical capture point) are illustrated with iso-surface maps in Figure 6. In the cation state of catalytic triad, the spin density was mainly distributed on the central imidazol ring (His), although a part of density was slightly distributed on Ser and Glu. This result indicates that the electron is

removed from HOMO of His after the ionization.

In the anion state, an excess electron was localized mainly on the imidazol ring (His) because the electron occupied the LUMO of His. The repulsive interaction between His^- and CH_3COO^-(Glu) was suddenly generated after the electron capture of [Ser-His-Glu]. Therefore, the dissociation of Glu occurred from $[His\text{-}Ser]^-$.

G. Comparison with CAS(5,5) and MP2 calculation

To check the effects of level of theory on the reaction dynamics, direct AIMD calculations were carried out using the MP2 and CAS(5,5) method with the 6-31G(d) basis set. Time evolutions of potential energies are plotted in Figure 7. All calculation showed the proton transfer from His^+ to Glu. The shapes of energy curve are in good agreement with each other. The rates of proton transfer from His^+ to Glu are summarized in Table 1. The MP2 calculation showed that the proton transfer takes place at 7.6 fs, which is in good agreement with that of the CAS(3,3) calculation (7.3 fs). Also, the CAS(5,5) method gave a close value (10.1 fs).

H. Summary of direct AIMD calculations

A total of five trajectories were run for both hole and electron capture processes. In hole capture process, all trajectories gave the proton transferred product. Also, the dissociation product was obtained in electro capture process. For example, another trajectory from the optimized structure was given in Figure S2 (hole capture) and Figure S3 (electron capture) in supporting information.

4. Discussion

A. Reaction model

On the basis of the present calculations, a reaction model for the radiation effect on the Ser-His-Glu catalytic triad is proposed in this section. Schematic illustration of the reaction model is given in Figure 8. We considered two radiation effects on the catalytic triad: ionization (hole capture) and electron attachment processes.

When the ionization takes place in the catalytic triad, a hole is mainly localized on His moiety in Ser-His-Glu. The hydrogen of His becomes a positive charge (proton-like). Subsequently, the proton transfer from His^+ to Glu spontaneously occurs.

If the catalytic triad accepts an excess electron, the unpaired electron is mainly localized on His, and negatively charged His is formed. The repulsive interaction between (His^-) and CH_3COO^-(Glu) in suddenly generated in [Ser-His-Glu]. This interaction causes a dissociation of Glu from the remaining part [Ser-His]. Thus, the skeleton structure of the catalytic triad is broken after the electron attachment to Ser-His-Glu. On the other hand, the skeleton structure is almost kept in ionization of catalytic triad, although the proton transfer takes place from His^+ to Glu.

B. Additional comments

In the present study, several approximations have been employed in the calculations of the potential energy surfaces. First, we assumed the CAS-SCF/6-31G(d) potential energy surface for the direct AIMD trajectory calculations. In previous papers [26-28], we investigated the reaction dynamics of several reaction systems using MP2 wave function. However, the MP2 wave function needs high cost, and was impossible to calculate the present catalytic triad because the present reaction system is very large for the MP2-dynamics calculation.

Therefore, we calculated only one trajectory with the MP2 method to obtain the validity of CAS(3,3) wave function. Both results were in good agreement with each other.

Second, tunnel effect is usually important in a proton transfer reaction. However, the present system occurs without activation barrier, so that the tunnel effect was not considered in the present system. Third, we neglected completely the effect of environmental media around Ser-His-Glu. The environmental media affects the activation barrier and electronic states of the catalytic triad. Therefore, it will be required in near feature that quantum mechanical and molecular mechanical (QM/MM) treatment are applied to the reaction system in order to obtain more realistic feature. Despite the several assumptions introduced here, the results enable us to obtain valuable information on the mechanism of the radiation effects in the Ser-His-Glu system.

Acknowledgment. The author acknowledges partial support from JSPS KAKENHI Grant Number 15K05371 and MEXT KAKENHI Grant Number 25108004.

Table 1. Rates of proton transfer from His^+ to Glu ($v(H^+)$ in fs) calculated by direct AIMD calculations.

Method	$v(H^+)$ / fs
CAS(3,3)	7.3
MP2	7.6
CAS(5,5)	10.1

References

(1) M.A. Santos, R.B. Faryabi, A.V. Ergen, A.M. Day, E. Callen, P. Gutierrez-Martinez, Nature, 514, 7520 (2014).

(2) A.G. Georgakilas, C.E. Redon, N.F. Ferguson, O.A. Martin, Cancer Lett. 353, 48-257 (2014).

(3) J. Yan, D. Tang, Expl. Cell Res. 328, 132-142 (2014).

(4) M.Y. Darensbourg, W. Weigand, Eur. J. Inorg. Chem., 7, 994-1004 (2011).

(5) S.P.J. Albracht, W. Roseboom, E.C. Hatchikian, J. Biol. Inorg. Chem., 1, 88-101 (2006).

(6) L. De Gioia, C. Elleouet, S. Munery, F.Y. Petillon, P. Schollhammer, J. Talarmin, G. Zampella, Eur. J. Inorg. Chem., 22, 3456-3461 (2014)

(7) J.W. Bourne, J.M. Lippell, P.A. Torzilli, Matrix Biol. 34, 179-184 (2014).

(8) H. Tachikawa, T. Fukuzumi, Phys. Chem. Chem. Phys.,13, 5881-5887 (2011).

(9) T. Schultz, E. Samoylova, W. Radloff, IV. Hertel, A.L. Sobolewski, W. Domcke, Science, 306, 1765-1768 (2004).

(10) P. Saravanaraman, C. Raj Kumar; R. Boopathy, J. Comput. Biol. 21, 632-647 (2014).

(11) C. Bartolucci, J. Stojan, Q.S.Yu, NH. Greig, D. Lamba, BioChem. J., 444, 269-277 (2012).

(12) J.Q. Araujo, J.A. Lima, A.D. Pinto, R.B. de Alencastro, M.G. Albuquerque, J. Mol. Model., 17, 1401-1412 (2011).

(13) Quinn, D. M. *Chem. Rev.*, *87*, 955-979 (1987).

(14) Dodson, G.; Wlodawer, A. *Trends Biochem. Sci.*, *23*, 347-352 (1998).

(15) Shafferman, A.; Kronman, C.; Flashner, Y.; Leitner, M.; Grosfeld, H.; Ordentlich, A.; Gozes, Y.; Cohen, S.; Ariel, N.; Barak, D.; Harel, M.; Silman, I.; Sussman, J. L.; Velan, B. *J. Biol. Chem.*, *267*, 17640-17648 (1992).

(16) Blow, D. M.; Birktoft, J. J.; Hartley, B. S. *Nature*, *221*, 337-340 (1969).

(17) Bachovchin, W. W.; Roberts, J. D. *J. Am. Chem. Soc.*, *100*, 8041-8047 (1978).

(18) Warshel, A.; Narayszabo, G.; Sussman, F.; Hwang, J. K. *Biochemistry*, *28*, 3629-3637 (1989).

(19) Fuxreiter, M.; Warshel, A. *J. Am. Chem. Soc.*, *120*, 183-194 (1998).

(20) Massiah, M. A.; Viragh, C.; Reddy, P. M.; Kovach, I. M.; Johnson, J.; Rosenberry, T. L.; Mildvan, A. S. *Biochemistry*, *40*, 5682-5690 (2001).

(21) Harel, M.; Quinn, D. M.; Nair, H. K.; Silman, I.; Sussman, J. L. *J. Am. Chem. Soc.*, *118*, 2340-2346 (1996).

(22) Li, G.-S,; Maigret, B.; Rinaldi, D.; Ruiz-Lopez, M.F., *J. Comput. Chem.* , *19*, 1675-1688 (1998).

(23) Zhang, Y,; Kua, J.; McCammon, J.A., *J. Am. Chem. Soc.*, *124*, 10572-10577 (2002).

(24) (T.california) Harel, M.; Quinn, D.M.; Nair, H.K.; Silman, L.; Sussman, J.L.; J. Am. Chem. Soc., 118, 2340-2346 (1996).

(25) M. J. Frisch, G. W. Trucks, H. B. Schlegel, G. E. Scuseria, M. A. Robb, J. R. Cheeseman, G. Scalmani, V. Barone, B. Mennucci, G. A. Petersson, H. Nakatsuji, M. Caricato, X. Li, H. P. Hratchian, A. F. Izmaylov, J. Bloino, G. Zheng, J. L. Sonnenberg, M. Hada, M. Ehara, K. Toyota, R. Fukuda, J. Hasegawa, M. Ishida, T. Nakajima, Y. Honda, O. Kitao, H. Nakai, T. Vreven, J. A. Montgomery, Jr., J. E. Peralta, F. Ogliaro, M. Bearpark, J. J. Heyd, E. Brothers, K. N. Kudin, V. N. Staroverov, R. Kobayashi, J. Normand, K. Raghavachari, A. Rendell, J. C. Burant, S. S. Iyengar, J. Tomasi, M. Cossi, N. Rega, J. M. Millam, M. Klene, J. E. Knox, J. B. Cross, V. Bakken, C. Adamo, J. Jaramillo, R. Gomperts, R. E. Stratmann, O. Yazyev, A. J. Austin, R. Cammi, C. Pomelli, J. W. Ochterski, R. L. Martin, K. Morokuma, V. G. Zakrzewski, G. A. Voth, P. Salvador, J. J. Dannenberg, S. Dapprich, A. D. Daniels, O. Farkas, J. B. Foresman, J. V. Ortiz, J. Cioslowski and D. J. Fox, Gaussian 09, Revision A.02, Gaussian, Inc., Wallingford CT, 2009.

(26) H. Tachikawa, J. Phys. Chem.A, 118, 3230-3236 (2014).

(27) H. Tachikawa, ChemPhysChem., 15, 1604-1610 (2014).

(28) H. Tachikawa, RSC Adv., 4, 516-522 (2014).

(29) M. J. Frisch, I. N. Ragazos, M. A. Robb, and H. B. Schlegel, Chem. Phys. Lett., 189, 524-28 (1992) .

(30) H. Tachikawa, T. Takada, Chem. Phys., 415, 76-83 (2013)

(31) Swope, William C.; H.C. Andersen, P.H. Berens, K.R. Wilson, J. Chem. Phys., 76, 648 (1982).

Figure captions

Figure 1. (Color online). Chemical structure of catalytic triad (Ser200-His440-Glu327), and optimized structure of model catalytic triad calculated at the MP2/6-311++G(d,p) level. Bond lengths and angles are in Å and in degree, respectively.

Figure 2. (Color online). Snapshots of $[Ser\text{-}His\text{-}Glu]^{+}$ after vertical ionization. Bond lengths and angles are in Å and in degree, respectively.

Figure 3. (Color online). Potential energy curves along the proton transfer coordinate.

Figure 4. (Color online). Snapshots of $[Ser\text{-}His\text{-}Glu]^{-}$ after vertical electron capture. Bond lengths and angles are in Å and in degree, respectively.

Figure 5. (Color online). Time evolution of potential energies of the reaction systems. Solid and dashed lines indicate the potential energy curves of $[Ser\text{-}His\text{-}Glu]^{+}$ and $[Ser\text{-}His\text{-}Glu]^{-}$, respectively.

Figure 6. (Color online). Spin density maps of of $[Ser\text{-}His\text{-}Glu]^{+}$ and $[Ser\text{-}His\text{-}Glu]^{-}$ at time zero.

Figure 7. (Color online). Time evolutions of potential energies of the reaction systems of $[Ser\text{-}His\text{-}Glu]^{+}$ after vertical ionization.

Figure 8. (Color online). Reaction model proposed in the present study.

Figure 1.

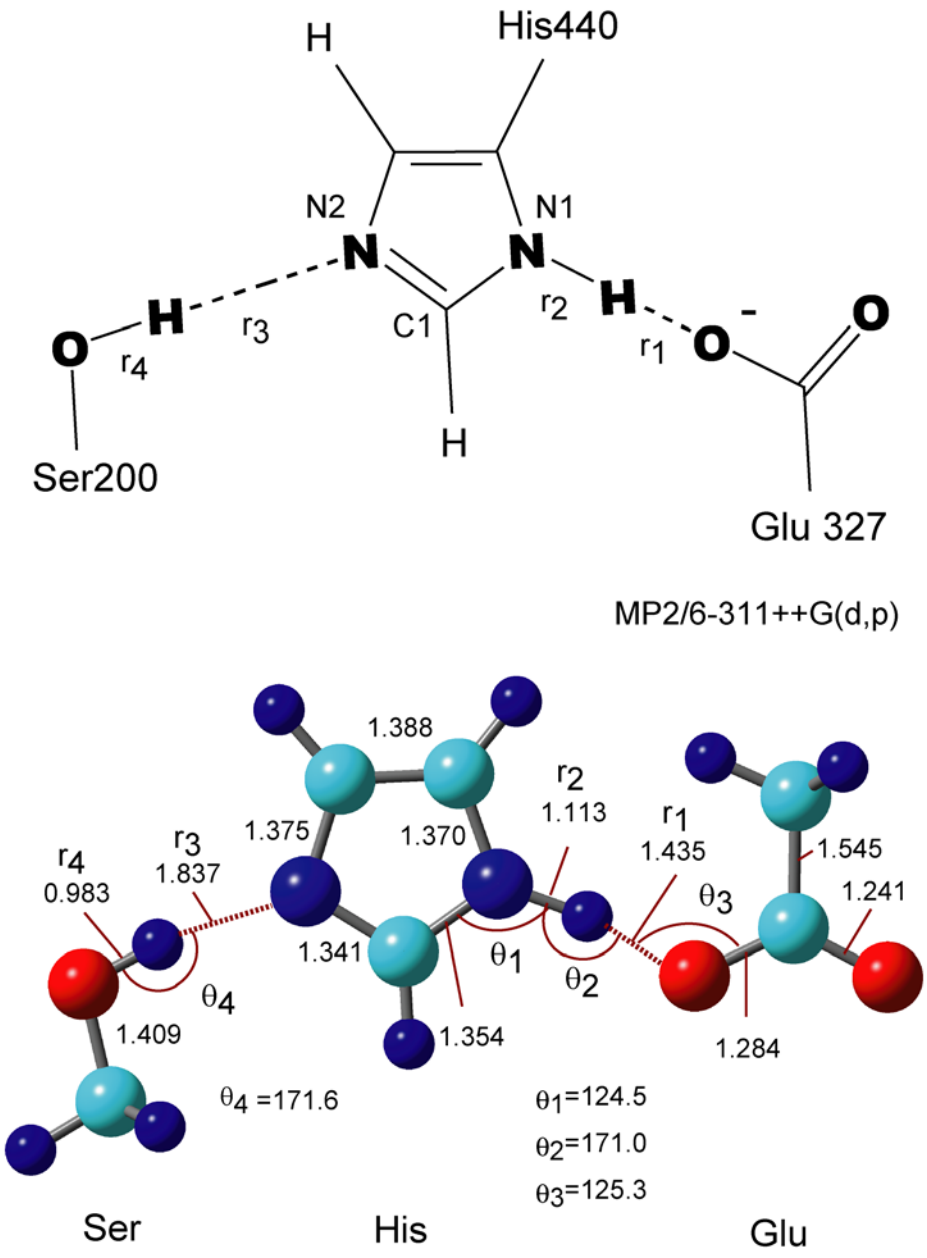
H
His440
N2
N1
N
N
C1
H
H
O
r4
r3
r2
r1
H
O
-
O
Ser200
Glu 327
MP2/6-311++G(d,p)
1.388
r2
1.113
r1
1.435
1.545
1.241
θ3
r4
0.983
r3
1.837
1.375
1.370
1.341
θ1
θ2
θ4
1.409
1.354
1.284
θ4 =171.6
θ1=124.5
θ2=171.0
θ3=125.3
Ser
His
Glu

Figure 2.

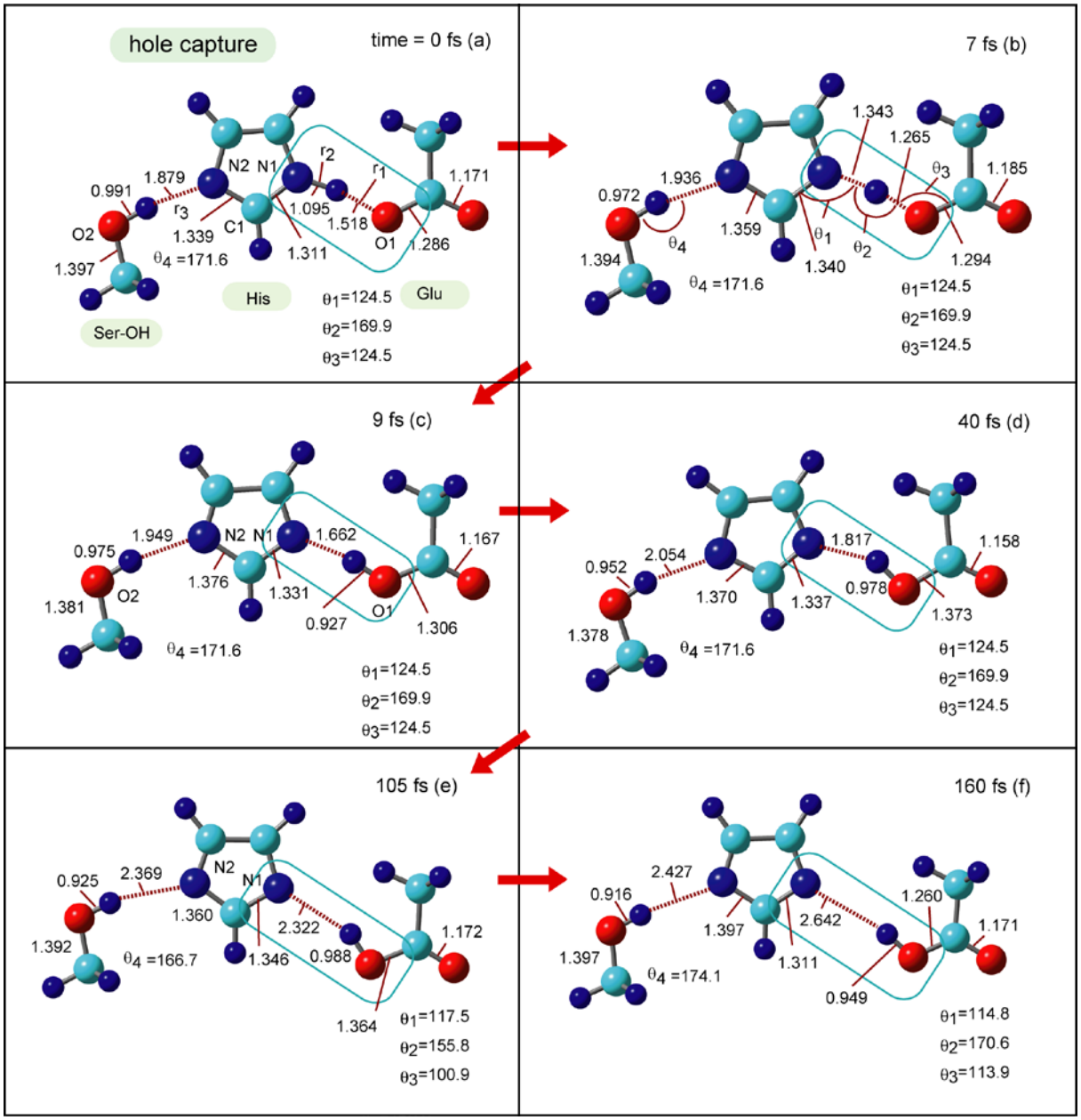
hole capture
time = 0 fs (a)
7 fs (b)
9 fs (c)
40 fs (d)
105 fs (e)
160 fs (f)
His
Glu
Ser-OH
N2
N1
C1
O1
O2
θ1=124.5
θ2=169.9
θ3=124.5
θ4 =171.6
θ1=117.5
θ2=155.8
θ3=100.9
θ4 =166.7
θ1=114.8
θ2=170.6
θ3=113.9
θ4 =174.1

Figure 3.

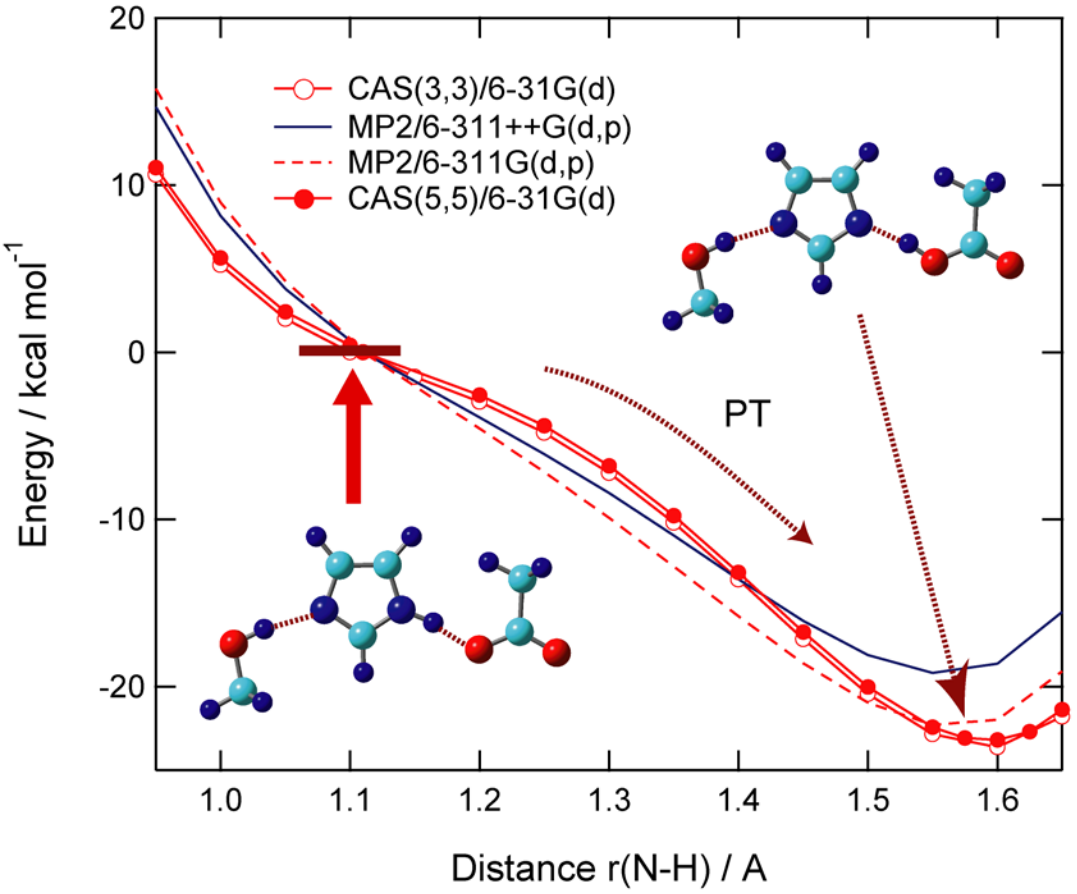
CAS(3,3)/6-31G(d)
MP2/6-311++G(d,p)
MP2/6-311G(d,p)
CAS(5,5)/6-31G(d)
PT
Energy / kcal mol-1
Distance r(N-H) / A
20
10
0
-10
-20
1.0
1.1
1.2
1.3
1.4
1.5
1.6

Figure 4.

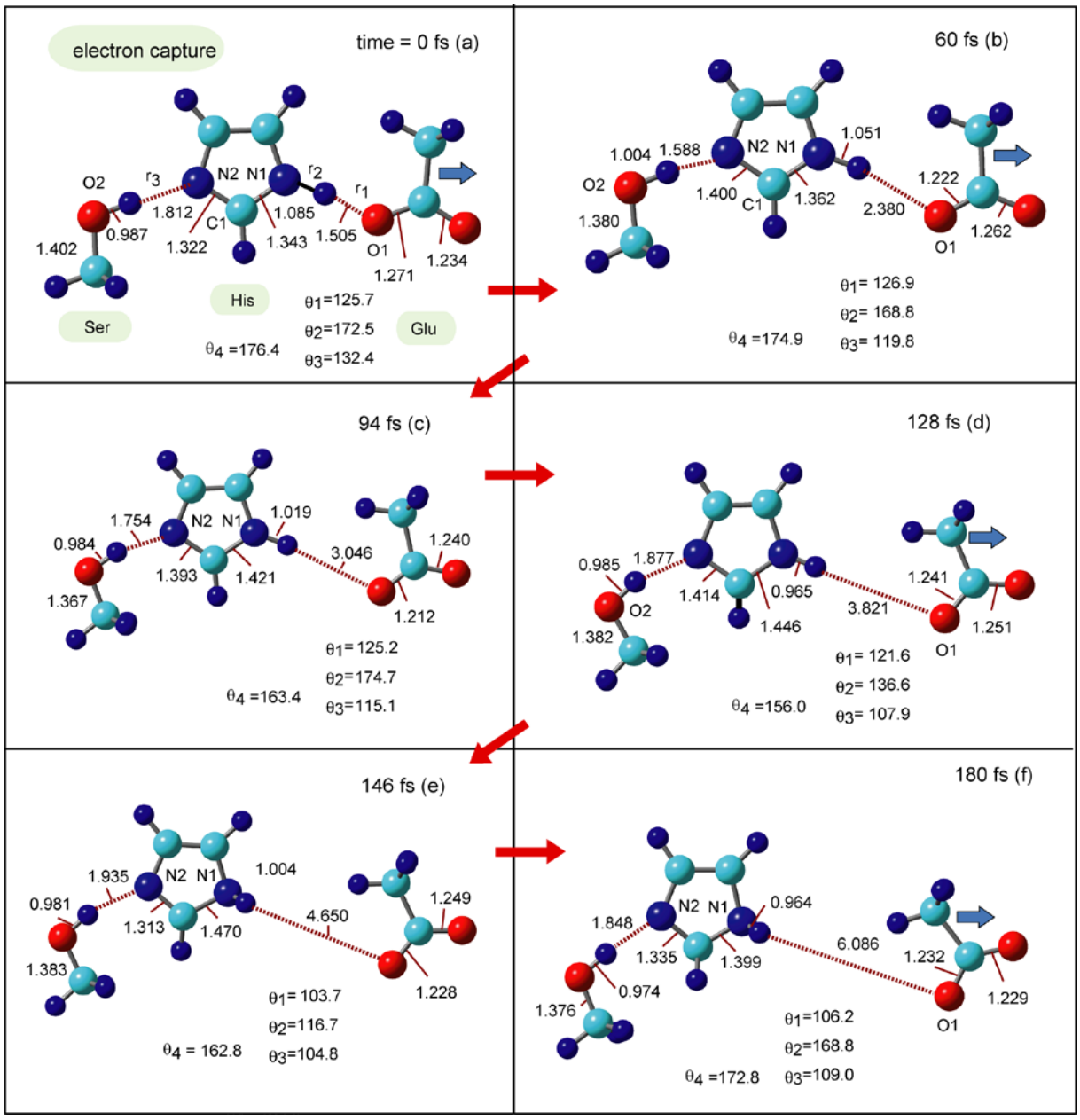
electron capture
time = 0 fs (a)
O2
r3
N2 N1
r2
r1
1.812
C1
1.085
0.987
1.322
1.343
1.505
O1
1.234
1.402
1.271
His
θ1=125.7
θ2=172.5
θ3=132.4
Ser
Glu
θ4 =176.4
60 fs (b)
1.004
1.588
N2 N1
1.051
O2
1.400
C1
1.362
1.222
2.380
1.380
1.262
O1
θ1= 126.9
θ2= 168.8
θ3= 119.8
θ4 =174.9
94 fs (c)
1.754
N2 N1
1.019
0.984
3.046
1.240
1.393
1.421
1.367
1.212
θ1= 125.2
θ2=174.7
θ3=115.1
θ4 =163.4
128 fs (d)
0.985
1.877
1.241
1.414
0.965
3.821
O2
1.446
1.251
1.382
O1
θ1= 121.6
θ2= 136.6
θ3= 107.9
θ4 =156.0
146 fs (e)
1.935
N2 N1
1.004
0.981
4.650
1.249
1.313
1.470
1.383
1.228
θ1= 103.7
θ2=116.7
θ3=104.8
θ4 = 162.8
180 fs (f)
1.848
N2 N1
0.964
6.086
1.232
1.335
1.399
0.974
1.229
1.376
O1
θ1=106.2
θ2=168.8
θ3=109.0
θ4 =172.8

Figure 5.

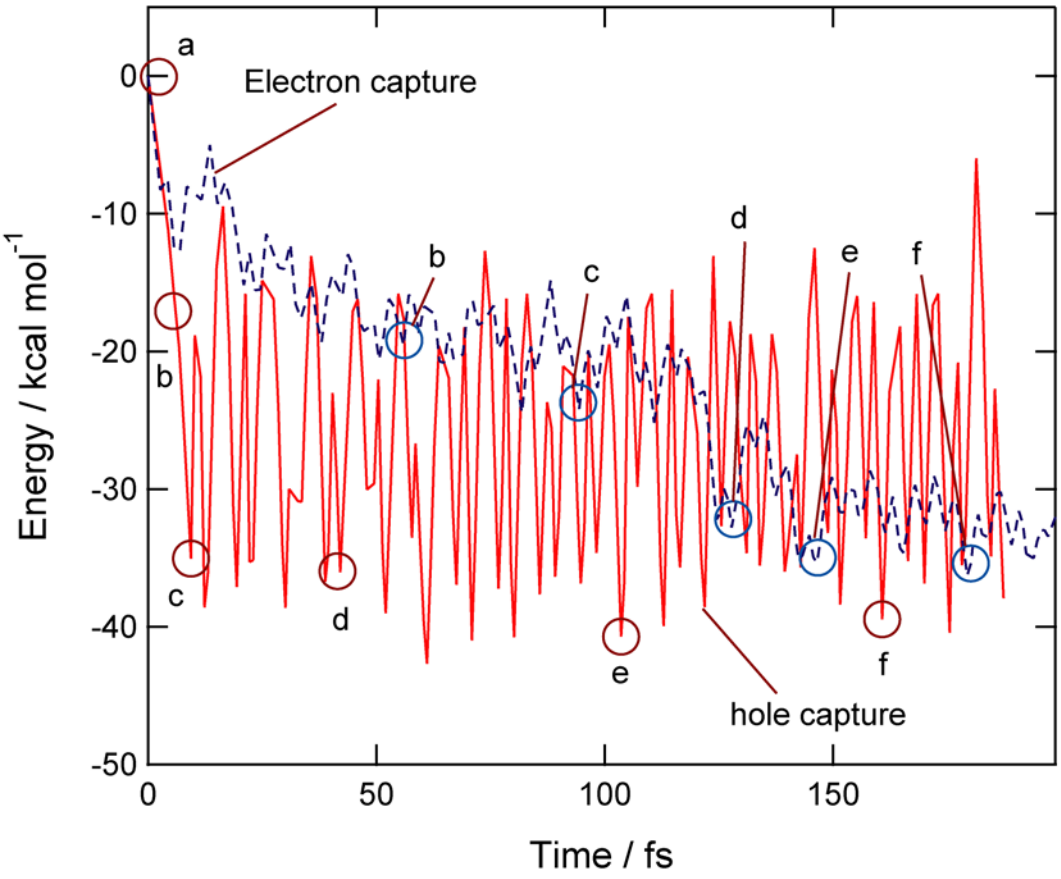
Energy / kcal mol-1
Time / fs
Electron capture
hole capture
a
b
c
d
e
f
0
-10
-20
-30
-40
-50
0
50
100
150

Figure 6

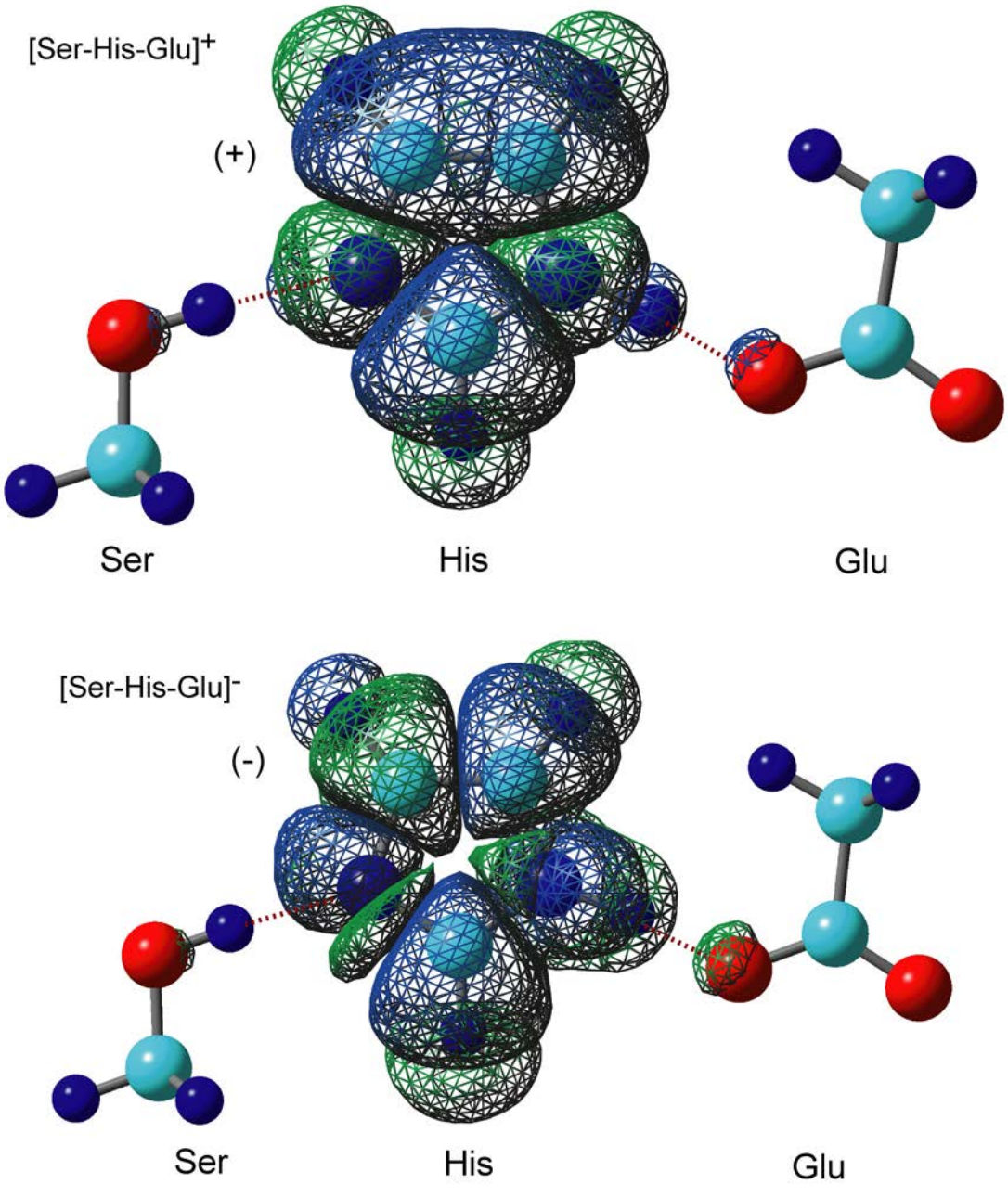

Figure 7.

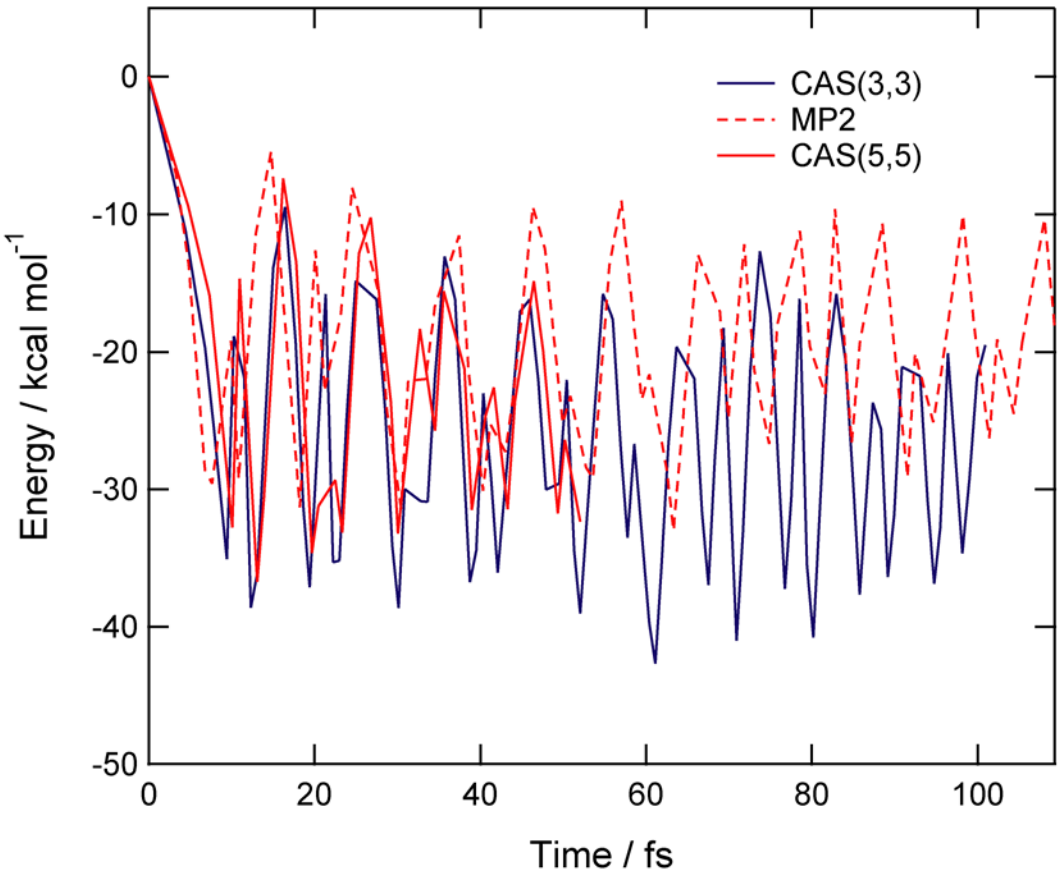
CAS(3,3)
MP2
CAS(5,5)
Energy / kcal mol-1
Time / fs
0
-10
-20
-30
-40
-50
0
20
40
60
80
100

Figure 8.

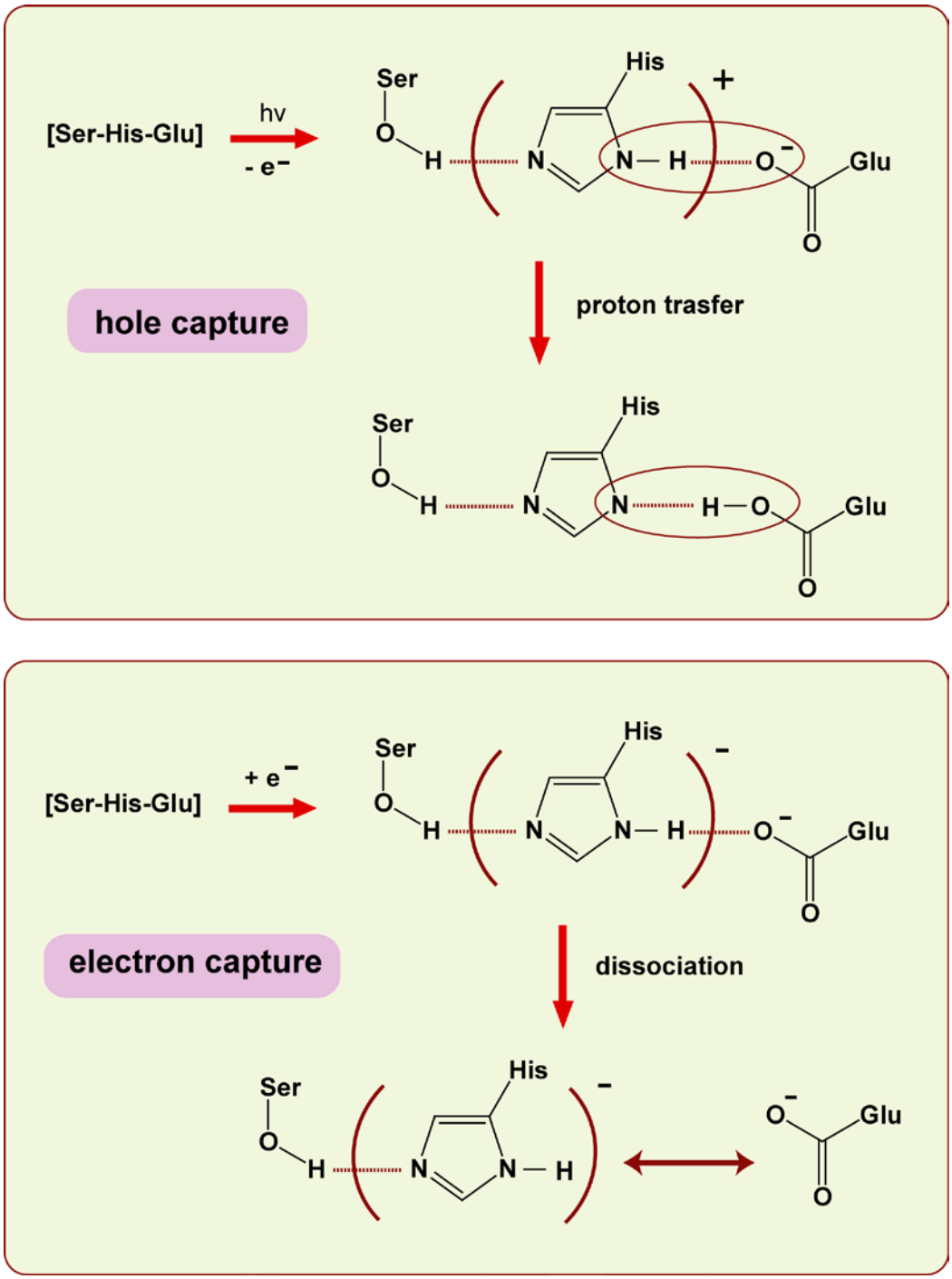
[Ser-His-Glu]
hv
- e⁻
Ser
His
Glu
hole capture
proton trasfer
+ e⁻
electron capture
dissociation